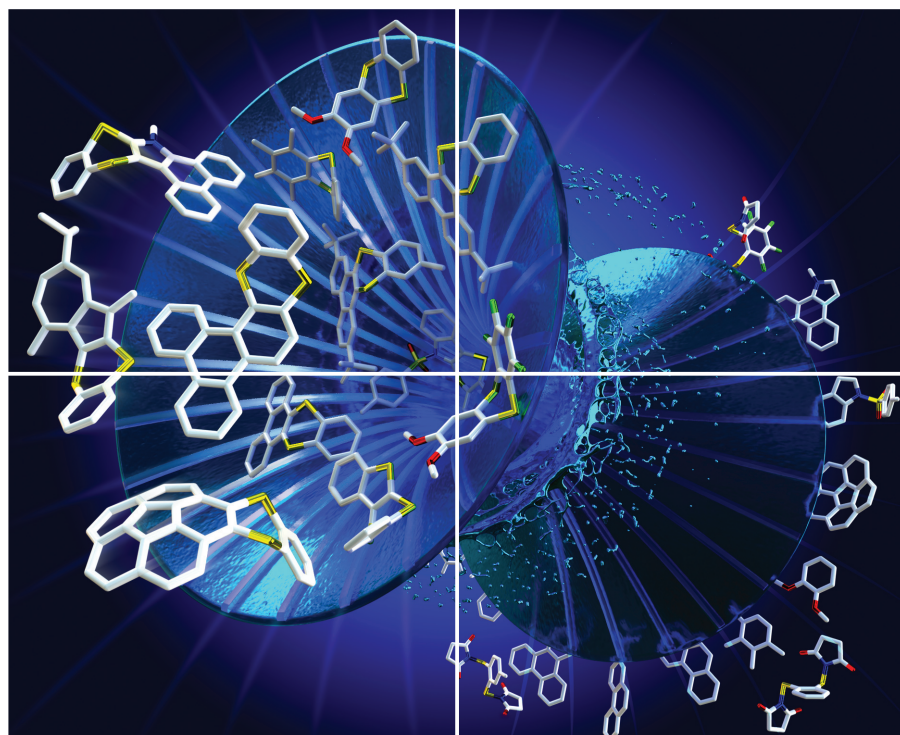


Volume 10 | Number 8 | 21 April 2023

**10**  
YEARS  
ANNIVERSARY



# ORGANIC CHEMISTRY

## FRONTIERS



CHINESE  
CHEMICAL  
SOCIETY



ROYAL SOCIETY  
OF CHEMISTRY

[rsc.li/frontiers-organic](https://rsc.li/frontiers-organic)

## RESEARCH ARTICLE

View Article Online

View Journal | View Issue

Cite this: *Org. Chem. Front.*, 2023, **10**, 1880

## One-step synthesis of polycyclic thianthrenes from unfunctionalized aromatics by thia-APEX reactions†

Kou P. Kawahara,<sup>a</sup> Hideto Ito <sup>\*a</sup> and Kenichiro Itami <sup>\*a,b</sup>

In this paper, thia-APEX reactions affording  $\pi$ -extended thianthrene derivatives from unfunctionalized aromatics are described. By utilizing *S*-diimidated 1,2-arenedithiols as benzene-1,2-dithiol dication synthons, new benzodithiine arms were fused to the unfunctionalized aromatic substrates in one step, affording  $\pi$ -extended thianthrenes in 21–87% yields. The present thia-APEX reaction occurs with equimolar amounts of aromatic substrates and *S*-diimidated 1,2-arenedithiols and a catalytic amount of TfOH, which is advantageous for the efficient creation of novel  $\pi$ -extended thianthrenes. In addition, the unique solid state packing structures and photophysical properties of the synthesized  $\pi$ -extended thianthrenes were elucidated in this study.

Received 1st January 2023,  
Accepted 13th February 2023

DOI: 10.1039/d2qo02058k

rsc.li/frontiers-organic

## Introduction

Thianthrene is a six-membered sulfur-containing heterocyclic compound consisting of a dibenzo-fused 1,4-dithiine ring in which two sulfur atoms are embedded diagonally (Fig. 1A).<sup>1</sup> Neutral thianthrene adopts a bent structure whose C–S–C angle is *ca.* 128°, whereas it reversibly transforms into a planar structure in the radical cation state.<sup>1c,2</sup> The redox behavior and cationic-state capability of thianthrene can be utilized for supramolecular chemistry<sup>2a,3</sup> and development of organic chemical reactions<sup>4</sup> and cathode materials.<sup>5</sup> Moreover, the thianthrene structure is favorable for electron-donation and inter-system crossing due to the electron-richness and heavy atom effect of sulfur atoms.<sup>6</sup> By utilizing these functionalities,  $\pi$ -extended thianthrenes have been developed in recent years.<sup>3–7</sup> Fig. 1B shows the representative thianthrene-based materials with unique reactivities and optoelectronic and supramolecular properties: room-temperature phosphorescence (compound A),<sup>6d</sup> thermally activated delayed fluorescence (TADF) (compound B),<sup>6d</sup> C–H functionalization of aromatic compounds (compound C),<sup>4</sup> semiconductivity (compound D),<sup>7l</sup> and host-guest capability for fullerenes (compound E).<sup>3</sup>

To meet the high demands of  $\pi$ -extended thianthrenes as functional molecules, easy and rapid synthetic methods are highly desired. Representative synthetic methods of thianthrene derivatives are shown in Fig. 2A. For example, symmetric thianthrene structures can be constructed utilizing arenethiols as starting materials with fuming H<sub>2</sub>SO<sub>4</sub> and reductants such as zinc and SnCl<sub>2</sub> (Fig. 2A-1).<sup>8</sup> Besides, using S<sub>2</sub>Cl<sub>2</sub> and Lewis acids such as AlCl<sub>3</sub>, symmetric thianthrenes can be directly synthesized from unfunctionalized aromatic substrates, while the applicable substrates are limited to simple

## (A) Structural features of thianthrenes

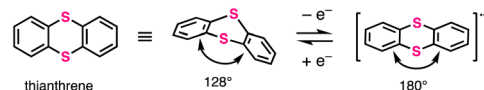
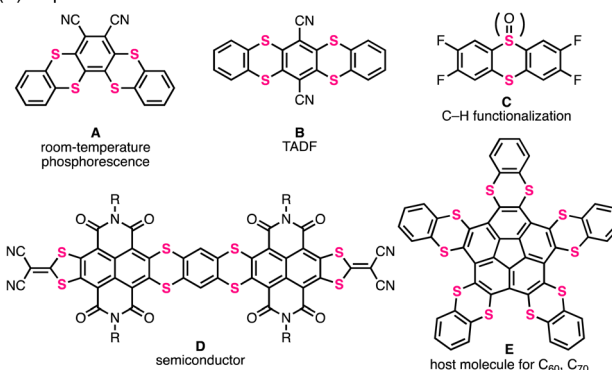
(B) Representative  $\pi$ -extended thianthrenes and their functions

Fig. 1  $\pi$ -Extended thianthrenes: structures, properties, and applications.

<sup>a</sup>Graduate School of Science, Nagoya University, Chikusa, Nagoya 464-8602, Japan

<sup>b</sup>Institute of Transformative Bio-Molecules (WPI-ITbM), Nagoya University, Chikusa, Nagoya 464-8602, Japan

†Electronic supplementary information (ESI) available: Syntheses, NMR, UV-vis absorption, emission, DFT calculations and crystallographic table. CCDC 2223785 (3ea), 2223786 (3eb) and 2241075 (3fa). For ESI and crystallographic data in CIF or other electronic format see DOI: <https://doi.org/10.1039/d2qo02058k>



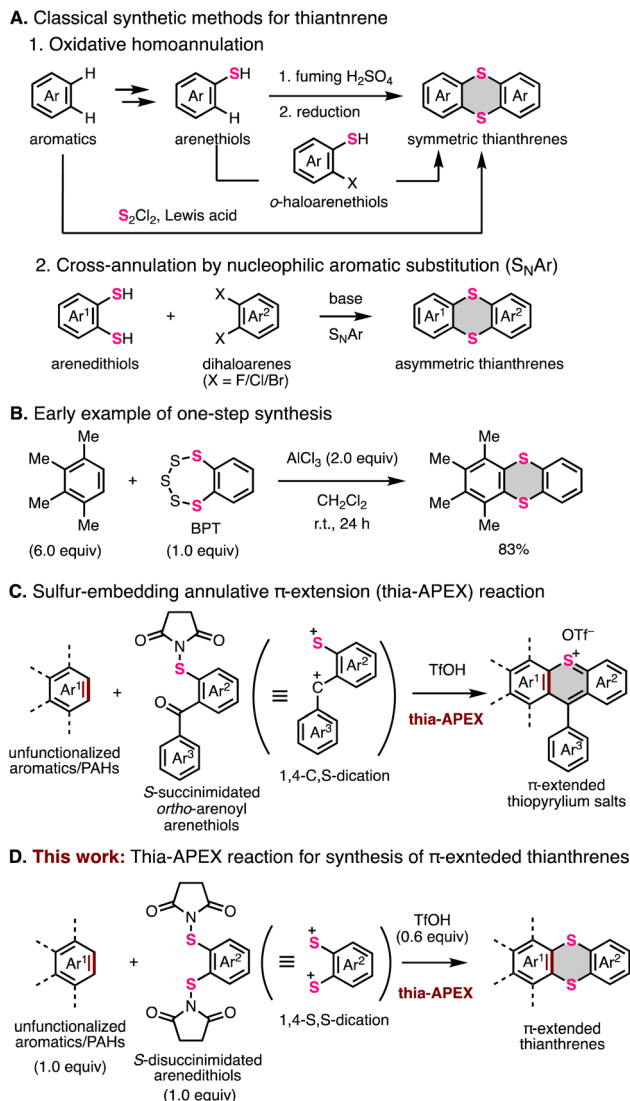


**Fig. 2** Conventional synthetic methods for thianthrenes and one-step synthesis using sulfur-embedding annulative  $\pi$ -extension (thia-APEX).

benzene derivatives.<sup>4b,9</sup> Alternatively,  $S_NAr$ -type homoannulation reactions using *ortho*-halogenated arenethiols and a base are also useful for the preparation of symmetric thianthrenes.<sup>10</sup> Furthermore, cross-annulation reactions using arylthiols and 1,2-dihaloarenes are frequently employed to construct unsymmetric thianthrene structures and large organic frameworks consisting of multiple thianthrene bridges (Fig. 2A-2).<sup>2c,5a,7c,e,h-k,11</sup> In this method, the characteristics of multistep transformations and the low availability of arene dithiols and dihaloarenes in larger aromatic systems would diminish the synthetic utility and efficiency of the whole synthetic process. One early example of one-step synthesis of thianthrenes was reported by Sato and coworkers in 1988 (Fig. 2B).<sup>12</sup> They used benzopentathiepin (BPT) and  $AlCl_3$  for cross-annulation of unfunctionalized arenes with a dithiine framework, achieving the one-step synthesis of various thianthrenes. However, this reaction requires excess amounts of

unfunctionalized aromatics to ensure a high yield. Due to this limitation, it seems difficult to apply it to the synthesis of larger aromatics. Therefore, the development of a more efficient and rapid synthetic method with a broad scope and applicability of substrates would be needed to advance the synthetic chemistry of thianthrenes.

Previously, we have devoted our efforts toward the development of a one-step annulative  $\pi$ -extension (APEX)<sup>13,14</sup> reaction and a heteroatom-embedding APEX (hetero-APEX)<sup>15</sup> reaction for efficient and rapid access to large polycyclic aromatic hydrocarbons (PAHs), polycyclic heteroaromatics and nanographenes from readily available unfunctionalized aromatics. Recently, we also developed a sulfur-embedding APEX (thia-APEX) reaction for the one-step synthesis of  $\pi$ -extended thiopyrylium salts (Fig. 2C).<sup>15o</sup> In this reaction, *S*-succinimidated *ortho*-arenyl arenethiols work as 1,4-*C,S*-dication  $\pi$ -extending agents in the presence of TfOH, and thus a one-step sequence of annulative C-S/C-C bond formation and dehydrative aromatization of unfunctionalized aromatics occurs with high regioselectivity. To further explore the potential of the thia-APEX strategy, we tested whether 1,2-arenedithiols having two succinimide groups will work as 1,4-*S,S*-dications, which would enable the one-step fusion of a benzodithiine ring onto unfunctionalized aromatics. Herein, we report a new thia-APEX reaction using *S*-diimidated 1,2-arenedithiols for the efficient one-step synthesis of  $\pi$ -extended thianthrenes under mild reaction conditions. Furthermore, some characteristic photophysical properties and structural features of the newly synthesized  $\pi$ -extended thianthrenes were elucidated by X-ray crystallographic analysis, measurements of absorption and emission, and density functional theory (DFT) calculations.

## Results and discussion

First, we newly prepared *S*-diimidated 1,2-benzenedithiol from 1,2-benzenedithiol (**2a**) (see the ESI† for details) and investigated the thia-APEX reaction of 1,2-dimethoxybenzene (**1a**) with **2a** as a  $\pi$ -extending agent (Table 1). When a mixture containing **1a** (0.20 mmol, 1.0 equiv.), **2a** (1.1 equiv.), and trifluoromethanesulfonic acid (TfOH, 2.3 equiv.) in 1,1,1,3,3,3-hexafluoroisopropyl alcohol (HFIP, 1.0 mL) was stirred at 80 °C under air for 13 h, the desired thia-APEX reaction proceeded to afford 2,3-dimethoxythianthrene (**3aa**) in 38% yield along with the demethylated by-product **4** in 25% yield (entry 1). The use of an excess amount of **2a** or a mixed solvent of 1,2-dichloroethane (DCE) and HFIP (v/v = 1 : 1) increased the yields of **3aa** with decreased formation of **4** (entries 2 and 3). The use of DCE alone as the solvent resulted in a higher yield than the use of HFIP as the solvent (entries 4–7). In this regard, the HFIP molecule or  $H_2O$  in HFIP might be involved in the deprotection of OMe to give **4**. To our delight, the use of a smaller amount of TfOH (*ca.* 0.6 equiv.) and a stoichiometric amount of **2a** was suitable for increasing the yield of product **3aa** (99% NMR yield, entry 7). The use of trifluoroacetic acid (TFA) instead of TfOH dramatically decreased the yield of



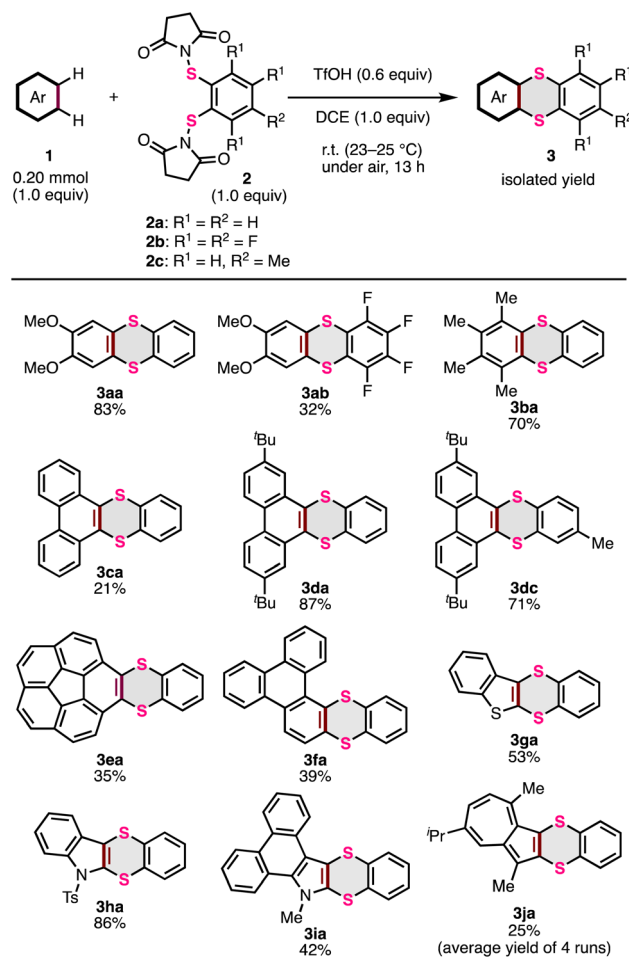
**Table 1** Optimization of the reaction conditions for the thia-APEX reaction of **1a** with **2a**

Entry	<b>2a</b> (equiv)	TfOH (equiv)	Solv.	Temp.	Yield of <b>3aa</b> <sup>a</sup>	Yield of <b>4</b> <sup>a</sup>
1	1.1	2.3	HFIP	80 °C	38% (38%)	16% (25%) <sup>c</sup>
2	2.0	2.5	HFIP	80 °C	57%	0%
3	1.0	2.4	DCE/HFIP <sup>b</sup>	80 °C	65%	17%
4	1.0	2.3	DCE	80 °C	71%	19%
5	1.0	1.1	DCE	80 °C	50%	26%
6	2.0	2.3	DCE	80 °C	65%	0%
7	1.0	0.64	DCE	80 °C	99% (78%)	0%
8 <sup>c</sup>	1.1	0.62 (TFA)	DCE	80 °C	3%	0%
9	1.0	2.2	DCE	100 °C	34%	25%
10	1.0	0.62	DCE	23 °C	>99% (83%)	0%

TfOH: trifluoromethanesulfonic acid; HFIP: 1,1,1,3,3,3-hexafluoroisopropyl alcohol; DCE: 1,2-dichloroethane; TFA: trifluoroacetic acid. <sup>a</sup> <sup>1</sup>H NMR yields determined using CH<sub>2</sub>Br<sub>2</sub> as the internal standard, and isolated yields in parentheses. <sup>b</sup> A mixed solvent of HFIP/DCE (v/v = 1 : 1) was used. <sup>c</sup> TFA was used instead of TfOH.

product **3aa**, implying the need for a strong acid for activating the S–N bonds (entry 8). Elevating the temperature to 100 °C resulted in an increased yield of **4** along with the decomposition of **3a** (entry 9). Finally, we found that the use of an equimolar amount of **1a** and **2a** in the presence of 0.6 equiv. of TfOH in DCE at room temperature (23 °C) are the best reaction conditions for the present thia-APEX reaction, and thus succeeded in exclusively obtaining **3aa** in 83% isolated yield (entry 10). Compared to the early report on one-step thianthrene synthesis by Sato,<sup>12</sup> the present thia-APEX reaction realized a 1 : 1 cross-annulation between the unfunctionalized arene and the  $\pi$ -extending agent with catalytic amounts of an acid even at room temperature.

With the optimized conditions in hand, the scope of thia-APEX reactions using other aromatic substrates was examined (Fig. 3). When using *S*-diimidated 3,4,5,6-tetrafluorobenzene-1,2-dithiol **2b** with **1a**, the thia-APEX reaction was less efficient, but afforded dimethoxytetrafluorothianthrene **3ab** in 32% yield. In the reaction with **2a**, 1,2,3,4-tetramethylbenzene (**1b**) was transformed to the corresponding thianthrene **3ba** in 70% yield. Unfortunately, the thia-APEX reactions of electron-deficient aromatic substrates such as 1,2-difluorobenzene and *ortho*-phthalodinitrile did not proceed, probably due to their lower nucleophilicities. Thianthrene **3ca** was also obtained in 21% yield from phenanthrene (**1c**) and **2a**. Although this reaction preferentially occurred at the *K*-region (C9, C10-position of phenanthrene: concave armchair edges in PAH), as same as the previous report,<sup>15a,o</sup> minor thia-APEX reactions at other regions and/or multi-thia-APEX reactions could result in lower yields of **3ca**. In contrast, the thia-APEX reaction using 2,7-di-

**Fig. 3** Scope of substrates in the thia-APEX reaction.

*tert*-butylphenanthrene (**1d**) with **2a** efficiently proceeded to afford dibenzothianthrene **3da** in 87% yield. Besides, by employing the methylated  $\pi$ -extending agent **2c** instead of compound **2a**, di-*tert*-butylphenanthrene **1d** was transformed to the corresponding dibenzothianthrene **3dc** in 71% yield. Thanks to the bulky *tert*-butyl groups, the  $\pi$ -extensions on other regions such as the C1–C2, C2–C3 and C3–C4 positions are considered to be prevented. Moreover, the thia-APEX reaction of C<sub>5v</sub>-symmetric corannulene (**1e**) with **2a** mainly afforded benzodithiine-fused corannulene **3ea** in 35% yield, although multi-thia-APEX products were also observed in the reaction mixture to some extent. Besides, benzodithiine-fused triphenylene **3fa** was obtained from pristine triphenylene (**1f**) in 39% yield. The structure of **3fa** was elucidated by X-ray crystallographic analysis (see the ESI†). In this reaction, there is a possibility of the formation of other regioisomers and multi-thia-APEX products, which can decrease the yield of **3fa**. Furthermore, benzo[*b*]thiophene (**1g**) and 1-tosyl-1*H*-indole (**1h**) were used as heteroaromatic templates for thia-APEX reactions, and dibenzodithiinothiophene **3ga** and dibenzodithiino-pyrrole **3ha** were obtained in 53% and 86% yields, respectively. Thia-APEX reactions also proceeded on unfunctionalized





heteroaromatic rings. For example, the thia-APEX reaction of *N*-methylindolizine **1i**, which was previously synthesized by us using the APEX reaction of *N*-methylpyrrole,<sup>14g</sup> with **2a** took place to afford **3ia** in 42% yield. Finally, guaiazulene (**1j**) was subjected to the thia-APEX conditions, and compound **3ja** was obtained in 25% yield (an average yield of four runs, see the ESI† for details) as a relatively unstable dark-green oil. In this reaction, the thia-APEX reaction selectively proceeded on the five-membered ring moiety.

Because new  $\pi$ -extended thianthrenes such as **3ca**, **3ea** and **3ja** were easily accessed by the thia-APEX reaction for the first time, the photophysical properties as well as the electronic structures of **3ca**, **3ea** and **3ja** were also investigated. First, dibenzothianthrene **3ca** showed an absorption band in the UV region, and the longest wavelength absorption maximum appeared at 331 nm in CH<sub>2</sub>Cl<sub>2</sub> (Fig. 4, green line). Thianthrene **3ca** emits strong blue-green fluorescence (fluorescence quantum yield ( $\Phi_F$ ) = 24%) upon excitation with 330 nm light, and the emission maximum was observed at 497 nm in CH<sub>2</sub>Cl<sub>2</sub> (Fig. 4, green dashed line). In the case of corannulene-fused thianthrene **3ea**, an intense absorption maximum and a weak shoulder peak were observed at 304 nm and at 350–450 nm, respectively (Fig. 4, orange line). Moreover, thianthrene **3ea** showed a broad fluorescence spectrum having a peak top at 560 nm (Fig. 4, orange dashed line) and an orange emission in CH<sub>2</sub>Cl<sub>2</sub>. Both thianthrene **3ca** and **3ea** showed Stokes shifts of *ca.* 160 nm, whose relatively large values were considered to be derived from large dynamic structural relaxations at their excited states.<sup>1,7j</sup> Furthermore, the fluorescence quantum yields of thianthrenes **3ca** and **3ea** were measured as 24% and 4%, respectively. Notably, the 24% quantum yield of **3ca** was even larger than those of pristine phenanthrene and triphenylene (*ca.* 10%),<sup>16</sup> which can be rationalized by the heavy atom effect of sulfur atoms and the prevention of

quenching of fluorescence by its bent structure.<sup>17</sup> Finally, we found that guaiazulene-fused benzodithiine **3ja** shows a green color in CH<sub>2</sub>Cl<sub>2</sub> and a weak and broad absorption band between 450–800 nm (Fig. S5†). This compound did not show fluorescence, which is strongly reflective of the nature of the guaiazulene core.

Next, the absorption properties and electronic structures of  $\pi$ -extended thianthrenes **3ca** and **3ea** were evaluated by DFT and time-dependent DFT (TD-DFT) calculations using the Gaussian 16 program<sup>18</sup> at the B3LYP/6-31+G(d,p) level of theory<sup>19</sup> and by consideration of the solvent effect using the integral equation formalism-polarizable continuum model (IEF-PCM)<sup>20</sup> in CH<sub>2</sub>Cl<sub>2</sub>. As shown in Fig. 5, the energy levels of the HOMO and LUMO of **3ca** were calculated to be −5.90 eV and −1.74 eV, respectively. While the HOMO of **3ca** is mainly localized on the 1,4-dithiine moiety, the LUMO of **3ca** is localized to some extent on the phenanthrene moiety. A similar HOMO and LUMO localization tendency was also found in **3ea**, and the energy levels of the HOMO and LUMO of **3ea** were calculated to be −5.96 eV and −2.20 eV, respectively. Compared with the HOMO and LUMO energy levels of pristine phenanthrene (HOMO: −6.12 eV; LUMO: −1.43 eV) and corannulene (HOMO: −6.35 eV; LUMO: −2.01 eV), the effect of

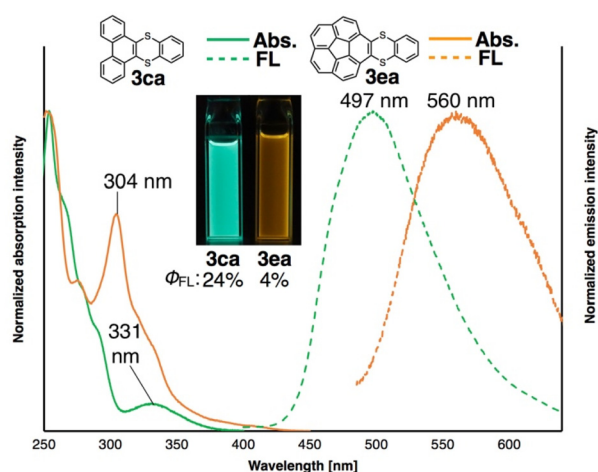


**Fig. 4** Absorption and emission spectra of  $\pi$ -extended thianthrenes **3ca** and **3ea** in CH<sub>2</sub>Cl<sub>2</sub>. Excitation wavelengths for fluorescence (FL) measurements: 330 nm (**3ca**) and 405 nm (**3ea**). The pictures of emission color were taken using the concentrated solutions of each compound under 365 nm of UV light irradiation.

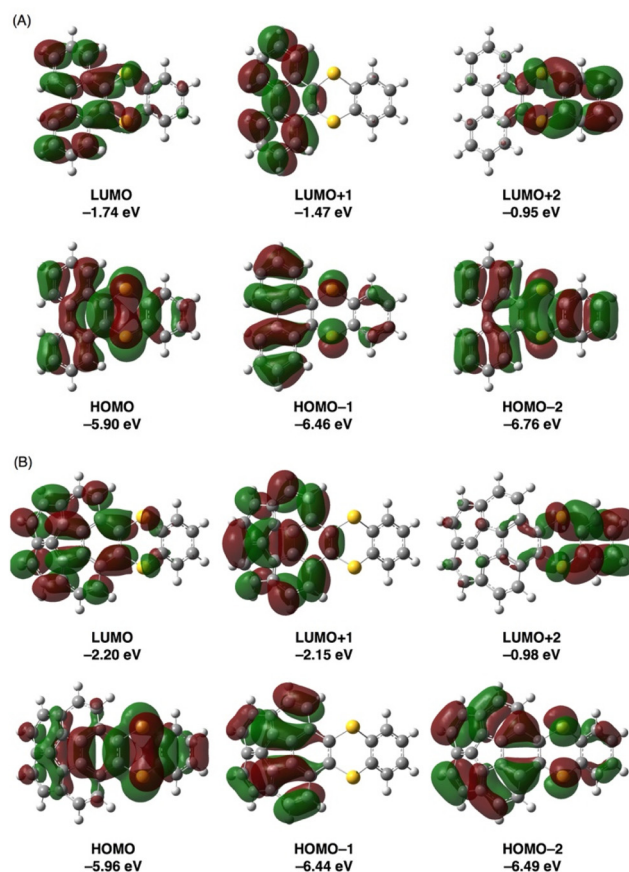


**Fig. 5** Representative frontier orbitals of **3ca** (A) and **3ea** (B) (isovalue = 0.02). Geometry optimization and energy calculations were conducted at the B3LYP/6-31+G(d,p) level of theory.



benzodithiine-fusion is slightly more predominant in increasing the energy levels of the HOMO ( $\Delta = +0.22$  and  $+0.39$  eV) rather than in decreasing those of the LUMO ( $\Delta = -0.31$  and  $-0.19$  eV). As a result, the HOMO–LUMO energy gaps of **3ca** and **3ea** are reduced by 0.53–0.58 eV compared with phenanthrene and corannulene. As shown in Table 2, the calculated excitation wavelength ( $\lambda_{\text{TD-DFT}}$ ) of the HOMO  $\rightarrow$  LUMO transition of thianthrene **3ca** was 347.21 nm ( $f = 0.0993$ ), which is consistent with the experimental longest wavelength absorption of **3ca** as a weak peak ( $\lambda_{\text{abs}} = 331$  nm). Besides, the second and third excitation attributed to HOMO  $\rightarrow$  LUMO+1 and HOMO–1  $\rightarrow$  LUMO transitions was calculated to be 334.84 nm ( $f = 0.0023$ ) and 299.47 nm ( $f = 0.2015$ ), respectively. The latter allowed excitation is considered to be the shoulder absorption peak around 290 nm. With regard to **3ea**, the electron transitions in three lowest energies were also estimated to be 395.93 nm ( $f = 0.0162$ , HOMO  $\rightarrow$  LUMO), 388.71 nm ( $f = 0.0229$ , HOMO  $\rightarrow$  LUMO+1) and 356.73 nm ( $f = 0.0000$ , HOMO–1  $\rightarrow$  LUMO+1), whose small or zero values of  $f$  show a good agreement with the weak shoulder absorptions between 350 to 450 nm. Moreover, the HOMO–1  $\rightarrow$  LUMO+1 transition ( $\lambda_{\text{TD-DFT}} = 356.73$  nm,  $f = 0.0000$ ) of **3ea** was determined as a forbidden transition.

Next, we performed the structural analyses of **3ca** and **3ea** by X-ray crystallographic analysis. Single crystals of **3ca** and **3ea** were obtained by recrystallization from chloroform/pentane by a vapor diffusion method. In the X-ray crystallographic analysis of **3ca**, two pairs of two molecules were observed in a unit cell, and both pairs consist of two molecules arranged in a pseudo- $C_2$ -symmetry, whose dithiine cores are directed in the same axis with *ca*.  $127^\circ$  bent angles (Fig. 6A). Each pair is directed in the opposite direction and positioned in a  $C_i$  symmetry, forming the two pseudo-enantiomeric pairs of two racemic molecules (Fig. 6A–C). Furthermore, each molecule is aligned in the direction of the *b* axis, forming columnar stacks, maintaining *ca*. 3.6 Å of intermolecular distance, which indicates weak  $\pi$ – $\pi$  interactions of **3ca** molecules.<sup>21</sup> This characteristic columnar packing is identical to that of unsubstituted thianthrene.<sup>22</sup> In the X-ray crystallographic analysis of **3ea**, the bent angle of the thianthrene moiety in **3ea** was found to be  $126^\circ$ , which is also closely identical to those of **3ca** and unsubstituted thianthrene (Fig. 6D).<sup>1,22</sup> Besides, the dangling benzodithiine arm is bent toward the concave face of the corannulene core, which forms a ladle-like shape. The one-dimen-

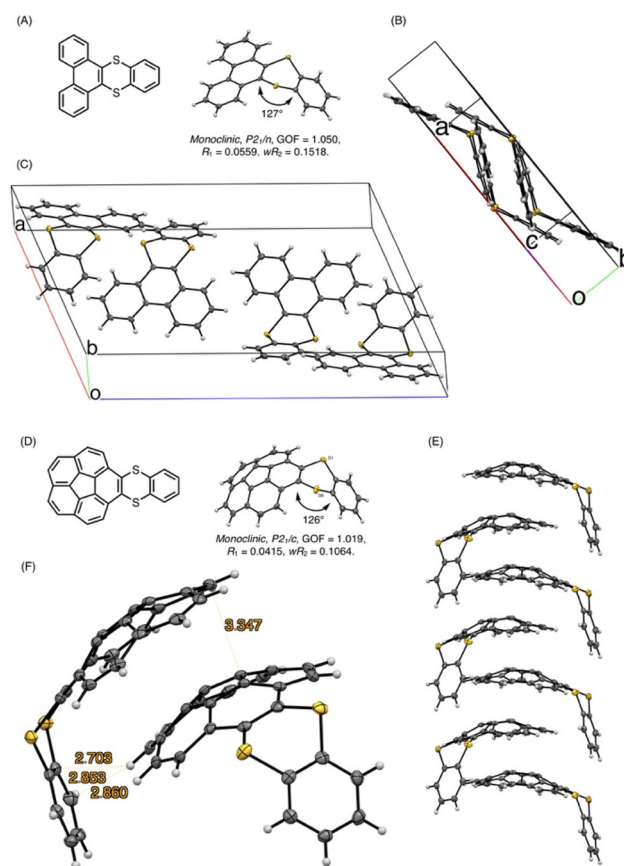


**Fig. 6** Structures of  $\pi$ -extended thianthrene **3ca**: (A) structure and ORTEP drawing of **3ca** with 50% probability, (B) side view of a unit cell, (C) top view of a unit cell, (D) structure and ORTEP drawing of **3ea** with 50% probability, (E) ORTEP drawing of the columnar packing structure of **3ea**, and (F) an extracted dimer structure with distances of  $\pi$ – $\pi$  and CH/ $\pi$  interaction in units of Å.

**Table 2** Results of TD-DFT calculations at the B3LYP/6-31+G(d,p) level of theory in  $\text{CH}_2\text{Cl}_2$  (IEF-PCM).  $\lambda_{\text{TD-DFT}}$ : estimated excitation wavelength;  $f$ : oscillator strength;  $\lambda_{\text{abs}}$ : the experimental observed longest wavelength absorption in  $\text{CH}_2\text{Cl}_2$

	$\lambda_{\text{TD-DFT}}$	$f$	Electronic transition (coefficient)	$\lambda_{\text{abs}}$
<b>3ca</b>	347.21 nm	0.0993	HOMO $\rightarrow$ LUMO (0.67256)	331 nm
	334.84 nm	0.0023	HOMO $\rightarrow$ LUMO+1 (0.61319)	—
	299.47 nm	0.2015	HOMO–1 $\rightarrow$ LUMO (0.56362)	—
<b>3ea</b>	395.93 nm	0.0162	HOMO $\rightarrow$ LUMO (0.68456)	350–450 nm
	388.71 nm	0.0229	HOMO $\rightarrow$ LUMO+1 (0.65994)	—
	356.73 nm	0.0000	HOMO–1 $\rightarrow$ LUMO+1 (0.61773)	—

sional columnar packings of **3ea** are aligned in an antiparallel manner to the neighboring molecular columns, counteracting the dipole moments of each column (Fig. 6E). Focusing on the distances between two neighboring molecules, each corannulene core is longitudinally aligned at 3.3 Å intervals, which are smaller than the sum of the van der Waals radii of two carbon atoms, indicative of the existence of the  $\pi$ – $\pi$  interaction.<sup>21</sup> Furthermore, the distances between the peripheral C–H bond in the corannulene core and the carbon atoms in the dangling benzene ring are less, and ranged from 2.7 to 2.9 Å. These values are within the sum of the van der Waals radii of one hydrogen and one carbon atom, showing the existence of CH/ $\pi$  interactions (Fig. 6F).<sup>23</sup> Depicting isosurfaces of non-covalent interaction (NCI) plot analysis using the NCIPLOT 4.0 program,<sup>24</sup> green isosurfaces, which indicate weak non-covalent interactions, are visually and clearly confirmed between the corannulene cores ( $\pi$ – $\pi$ ) and between the corannulene core and the benzene ring (CH/ $\pi$ ) (Fig. 7). Because unsubstituted corannulene in the solid state shows a disordered arrangement derived from CH/ $\pi$  interactions, the thianthrene arms are considered to contribute to the formation of the



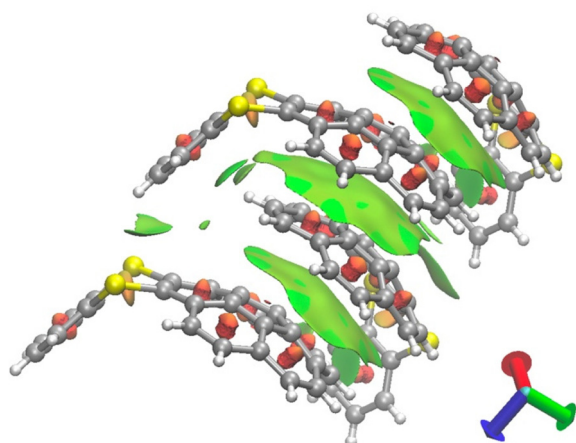


**Fig. 7** NCI analysis and reduced density gradient isosurface (isosurface value = 0.3) using the NCIPLOT4 program for  $\pi$ -extended thianthrene **3ea**. Color code based on sign ( $\lambda_2$ )  $\rho$  was:  $-0.07$  a.u. (blue)  $< 0.0$  a.u. (green)  $< 0.07$  a.u. (red). Blue and red isosurfaces show regions having attractive and repulsive interactions, respectively, and green isosurfaces show weak van der Waals interactions such as  $\pi$ - $\pi$  interaction. The structure of **3ea** was extracted from the data of X-ray crystallographic analysis.

columnar packing structure. In addition, the columnar packing structure of thianthrene **3ea** is the first example of mono-benzodithiine-fused corannulene,<sup>3,7e</sup> whereas there are a lot of other *rim*-region-fused or *rim*-region-substituted corannulene derivatives showing a similar columnar stacking ability.<sup>25</sup> We expect that the columnar stacking achieved by the simple structural motif of benzodithiinocorannulene can provide a fruitful insight into the application of corannulene-based functional materials in organic electronics<sup>26</sup> and supramolecular chemistry<sup>27</sup> as well as host-guest chemistry.<sup>3</sup>

To obtain insights into the bent structures of thianthrenes **3ca** and **3ea** in crystalline and solution states, their inversion barriers were examined using DFT calculations. The structures of thianthrenes **3ca** and **3ea** in the ground and transition states were optimized at the B3LYP/6-31+G(d,p) level of theory. **3ca** has only one stable bent structure (see the ESI†), whereas **3ea** has two stable structures, a ladle-shaped one (**3ea-ladle**) and a spoon-shaped one (**3ea-spoon**), because of the inversion of the corannulene core and the benzodithiine arm (Fig. 8). **3ea-ladle** was the most stable conformer in **3ea**, whose structure was also observed by X-ray crystallographic analysis (Fig. 6). The inversion barriers corresponding to the inversion of benzodithiine arms were calculated to be  $7.31 \text{ kcal mol}^{-1}$  for **TS1**<sub>3ca</sub> and  $7.47 \text{ kcal mol}^{-1}$  for **TS1**<sub>3ea</sub>. The values of **TS1**<sub>3ca</sub> and **TS1**<sub>3ea</sub> are larger than that of pristine thianthrene ( $5.1 \text{ kcal mol}^{-1}$ , at the B3LYP/6-31+G(d,p) level),<sup>28</sup> indicating that the PAH structures of phenanthrene and corannulene make the inversion barriers of benzodithiine arms higher. Furthermore, the transition state of corannulene core flipping in **3ea** (**TS2**<sub>3ea</sub>) was optimized and its barrier was calculated to be  $9.72 \text{ kcal mol}^{-1}$ . This value is also closely identical to that of pristine corannulene.<sup>29</sup> In conclusion, newly synthesized **3ca** and **3ea**

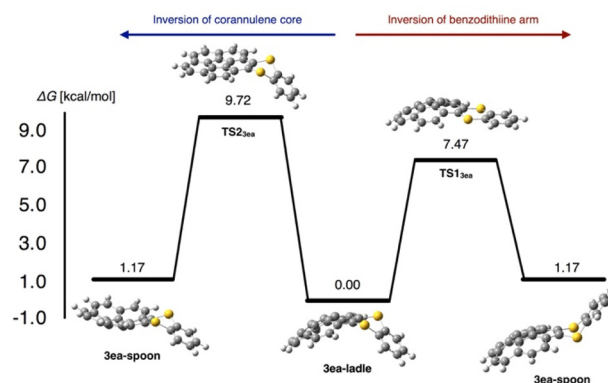


**Fig. 8** Two possible pathways of the structural inversion of thianthrene **3ea** and their calculated barrier at the B3LYP/6-31+G(d,p) level of theory.

were found to be hybrid molecules of thianthrene and PAHs. Their bent structures and conformational changes reflect the nature of both thianthrene and PAH cores well.

## Conclusions

By using *S*-diimidated 1,2-benzenedithiol derivatives as new  $\pi$ -extending agents, thianthrenes and  $\pi$ -extended thianthrenes were efficiently obtained by the thia-APEX reaction of unfunctionalized aromatic substrates in one step. In addition, the characteristic photophysical and electronic properties and structural features of thia-APEX products were elucidated by UV-vis absorption and emission spectroscopy, DFT calculations and X-ray crystallographic analysis. In particular, the  $\pi$ -extended thianthrenes having phenanthrene and corannulene cores (**3ca** and **3ea**) showed emission properties with larger Stokes shifts. **3ca** showed higher fluorescence quantum yields than pristine phenanthrene and triphenylene. Regarding corannulene-fused thianthrene **3ea**, 1D-columnar packing in the solid state was observed, which is in stark contrast to pristine corannulene. The newly developed thia-APEX reaction is expected to contribute to the rapid and efficient creation of unique  $\pi$ -extended thianthrenes having various aromatic cores.

## Conflicts of interest

There are no conflicts to declare.

## Acknowledgements

This work was supported by the JST-CREST program (JPMJCR19R1 to H. I.), the JSPS KAKENHI (JP19H05463 to K. I., JP20K21192 and JP21H01931 to H. I.), and the Noguchi Research Foundation and the Foundation of Public Interest of





Tatematsu (to H. I.). K. P. K. gratefully acknowledges the JSPS Research Fellowship for Young Scientists (DC1). We thank Mr. Hiroki Shudo for helping with the X-ray crystallographic analysis and taking pictures of sample solutions. NMR spectroscopy and MS measurements were conducted using resources from the Chemical Instrumentation Facility (CIF), Research Center for Materials Science (RCMS), and Institute of Transformative Bio-Molecules (ITbM), Nagoya University. Calculations were performed using the resources of the Research Center for Computational Science, Okazaki, Japan (Projects: 21-IMS-C070 and 22-IMS-C069) and the SuperComputer System, Institute for Chemical Research, Kyoto University.

## References

- (a) K. Kobayashi and C. L. J. Gajurel, The Chemistry of 1, 4-Dithiins, *Sulphur Chem.*, 1986, **7**, 123; (b) S. I. Etkind and T. M. Swager, The Properties, Synthesis, and Materials Applications of 1,4-Dithiins and Thianthrenes, *Synthesis*, 2022, **54**, 4843; (c) K. L. Gallaher and S. H. Bauer, Structure and inversion potential of thianthrene, *J. Chem. Soc., Faraday Trans. 2*, 1975, **71**, 1173; (d) K. Kobayashi, Chemistry of 1, 4-dithiins, *J. Synth. Org. Chem., Jpn.*, 1982, **40**, 642; (e) A. Ito, H. Ino, H. Ichiki and K. Tanaka, Tuning Spin-State Preference by Substituents: A Case Study of Thianthrene Dication, *J. Phys. Chem. A*, 2002, **106**, 8716.
- (a) J. Yuan, W. Lv, A. Li and K. Zhu, A self-assembled M2L2 truncated square and its application as a container for fullerenes, *Chem. Commun.*, 2021, **57**, 12848; (b) M. Yamashita, H. Hayashi, M. Suzuki, D. Kuzuhara, J. Yuasa, T. Kawai, N. Aratani and H. Yamada, Bisanthra-thianthrene: synthesis, structure and oxidation properties, *RSC Adv.*, 2016, **6**, 70700; (c) S. Tang, L. Zhang, H. Ruan, Y. Zhao and X. Wang, A Magnetically Robust Triplet Ground State Sulfur-Hydrocarbon Diradical Dication, *J. Am. Chem. Soc.*, 2020, **142**, 7340; (d) D. Casarini, C. Coluccini, L. Lunazzi and A. Mazzanti, *J. Org. Chem.*, 2006, **71**, 6248; (e) W. J. Ong, F. Bertani, E. Dalcanele and T. M. Swager, Redox Switchable Thianthrene Cavitands, *Synthesis*, 2017, **49**, 358.
- (a) M. Bancu, A. K. Rai, P. Cheng, R. D. Gilardi and L. T. Scott, Corannulene Polysulfides: Molecular Bowls with Multiple Arms and Flaps, *Synlett*, 2004, 173; (b) P. E. Georghiou, A. H. Tran, S. Mizyed, M. Bancu and L. T. Scott, Concave polyarenes with sulfide-linked flaps and tentacles: new electron-rich hosts for fullerenes, *J. Org. Chem.*, 2005, **70**, 6158.
- (a) H. Meng, M.-S. Liu and W. Shu, Organothianthrenium salts: synthesis and utilization, *Chem. Sci.*, 2022, **13**, 13690; (b) F. Berger, M. B. Plutschack, J. Riegger, W. Yu, S. Speicher, M. Ho, N. Frank and T. Ritter, Site-selective and versatile aromatic C–H functionalization by thianthrenation, *Nature*, 2019, **567**, 223; J. Chen, J. Li, M. B. Plutschack, F. Berger and T. Ritter, Regio- and Stereoselective Thianthrenation of Olefins To Access Versatile Alkenyl Electrophiles, *Angew. Chem., Int. Ed.*, 2020, **59**, 5616; (c) H. Jia and T. Ritter,  $\alpha$ -Thianthrenium Carbonyl Species: The Equivalent of an  $\alpha$ -Carbonyl Carbocation, *Angew. Chem., Int. Ed.*, 2022, **61**, e202208978; (d) H. Jia, A. P. Häring, F. Berger, L. Zhang and T. Ritter, Trifluoromethyl Thianthrenium Triflate: A Readily Available Trifluoromethylating Reagent with Formal  $\text{CF}_3^+$ ,  $\text{CF}_3^\cdot$ , and  $\text{CF}_3^-$  Reactivity, *J. Am. Chem. Soc.*, 2021, **143**, 7623; (e) F. Juliá, Q. Shao, M. Duan, M. B. Plutschack, F. Berger, J. Mateos, C. Lu, X.-S. Xue, K. N. Houk and T. Ritter, High Site Selectivity in Electrophilic Aromatic Substitutions: Mechanism of C–H Thianthrenation, *J. Am. Chem. Soc.*, 2021, **143**, 16041; (f) F. Juliá, J. Yan, F. Paulus and T. Ritter, Vinyl Thianthrenium Tetrafluoroborate: A Practical and Versatile Vinylating Reagent Made from Ethylene, *J. Am. Chem. Soc.*, 2021, **143**, 12992; (g) D. E. Holst, D. J. Wang, M. J. Kim, I. A. Guzei and Z. K. Wickens, Aziridine synthesis by coupling amines and alkenes via an electrogenerated dication, *Nature*, 2021, **596**, 74; (h) D. J. Wang, K. Targos and Z. K. Wickens, *J. Am. Chem. Soc.*, 2021, **143**, 21503; (i) Y. Xiong, X. Zhang, H.-M. Guo and X. Wu, Photoredox/persistent radical cation dual catalysis for alkoxy radical generation from alcohols, *Org. Chem. Front.*, 2022, **9**, 3532.
- (a) S. Haldar, M. Wang, P. Bhauriyal, A. Hazra, A. H. Khan, V. Bon, M. A. Isaacs, A. De, L. Shupletsov, T. Boenke, J. Grothe, T. Heine, E. Brunner, X. Feng, R. Dong, A. Schneemann and S. Kaskel, Porous Dithiine-Linked Covalent Organic Framework as a Dynamic Platform for Covalent Polysulfide Anchoring in Lithium–Sulfur Battery Cathodes, *J. Am. Chem. Soc.*, 2022, **144**, 9101; (b) M. Fu, C. Zhang, Y. Chen, K. Fan, G. Zhang, J. Zou, Y. Gao, H. Dai, X. Wang and C. Wang, A thianthrene-based small molecule as a high-potential cathode for lithium–organic batteries, *Chem. Commun.*, 2022, **58**, 11993; (c) M. Yao, N. Taguchi, H. Ando, N. Takeichi and T. Kiyobayashi, Improved gravimetric energy density and cycle life in organic lithium-ion batteries with naphthazarin-based electrode materials, *Commun. Mater.*, 2020, **1**, 70.
- (a) P. Pander, A. Swist, R. Turczyn, S. Pouget, D. Djurado, A. Lazauskas, R. Pashazadeh, J. V. Grazulevicius, R. Motyka, A. Klimash, P. J. Skabara, P. Data, J. Soloducho and F. B. Dias, Observation of Dual Room Temperature Fluorescence–Phosphorescence in Air, in the Crystal Form of a Thianthrene Derivative, *J. Phys. Chem. C*, 2018, **122**, 24958; (b) Y. Wen, H. Liu, S.-T. Zhang, G. Pan, Z. Yang, T. Lu, B. Li, J. Cao and B. Yang, Modulating Room Temperature Phosphorescence by Oxidation of Thianthrene to Achieve Pure Organic Single-Molecule White-Light Emission, *CCS Chem.*, 2020, **2**, 1940; (c) Z. Yang, S. Zhao, X. Zhang, M. Liu, H. Liu and B. Yang, Efficient Room-Temperature Phosphorescence from Discrete Molecules Based on Thianthrene Derivatives for Oxygen Sensing and Detection, *Front. Chem.*, 2022, **9**, 810304; (d) M. Li, W. Xie, X. Cai, X. Peng, K. Liu, Q. Gu,





- J. Zhou, W. Qiu, Z. Chen, Y. Gan and S.-J. Su, Molecular Engineering of Sulfur-Bridged Polycyclic Emitters Towards Tunable TADF and RTP Electroluminescence, *Angew. Chem., Int. Ed.*, 2022, **61**, e202209343; (e) J. Chen, H. Tian, Z. Yang, J. Zhao, Z. Yang, Y. Zhang, M. P. Aldred and Z. Chi, A Multi-Stimuli-Responsive Molecule with Responses to Light, Oxygen, and Mechanical Stress through Flexible Tuning of Triplet Excitons, *Adv. Opt. Mater.*, 2021, **9**, 2001550; (f) A. Tomkeviciene, T. Matulaitis, M. Guzauskas, V. Andruleviciene, D. Volyniuk and J. V. Grazulevicius, Thianthrene and acridan-substituted benzophenone or diphenylsulfone: Effect of triplet harvesting via TADF and phosphorescence on efficiency of all-organic OLEDs, *Org. Electron.*, 2019, **70**, 227.
- 7 Representative applications of ( $\pi$ -extended) thianthrenes: (a) A. Bartl and J. Fröhner, New charge-transfer complexes with polyconjugated sulfur compounds, *Synth. Met.*, 1992, **51**, 115; (b) B. Fiedler, E. Rojo-Wiechel, J. Klassen, J. Simon, J. Beck and M. Sokolowski, Ordered structures of two sulfur containing donor molecules on the Au(111) surface, *Surf. Sci.*, 2012, **606**, 1855; (c) Z. Liu, W. Wang, W. Xu, H. Chen, X. Zhang, T. Ren, X. Wang, J. Zhao and J. Xiao, Synthesis, characterization and photocurrent behavior of asymmetrical heterotwistacenes, *Dyes Pigm.*, 2015, **115**, 143; (d) P. A. Denis, Theoretical characterization of existing and new fullerene receptors, *RSC Adv.*, 2013, **3**, 25296; (e) V. Barát, M. Budanović, D. Halilović, J. Huh, R. D. Webster, S. H. Mahadevegowda and M. C. Stuparu, A general approach to non-fullerene electron acceptors based on the corannulene motif, *Chem. Commun.*, 2019, **55**, 3113; (f) T. Ren, J. Xiao, W. Wang, W. Xu, S. Wang, X. Zhang, X. Wang, H. Chen, J. Zhao and L. Jiang, Synthesis, Crystal Structures, Optical Properties, and Photocurrent Response of Heteroacene Derivatives, *Chem. – Asian J.*, 2014, **9**, 1943; (g) S. Riebe, S. Adam, B. Roy, I. Maisuls, C. G. Daniliuc, J. Dubbert, C. A. Strassert, I. Schapiro and J. Voskuhl, Bridged Aromatic Oxo- and Thioethers with Intense Emission in Solution and the Solid State, *Chem. – Asian J.*, 2021, **16**, 2307; (h) S. I. Etkind, J. Lopez, Y. G. Zhu, J.-H. Fang, W. J. Ong, Y. Shao-Horn and T. M. Swager, Thianthrene-Based Bipolar Redox-Active Molecules Toward Symmetric All-Organic Batteries, *ACS Sustainable Chem. Eng.*, 2022, **10**, 11739; (i) Z. Nelson, L. Delage-Laurin, M. D. Peeks and T. M. Swager, Large Faraday Rotation in Optical-Quality Phthalocyanine and Porphyrin Thin Films, *J. Am. Chem. Soc.*, 2021, **143**, 7096; (j) W. J. Ong and T. M. Swager, Dynamic self-correcting nucleophilic aromatic substitution, *Nat. Chem.*, 2018, **10**, 1023; (k) T. Jin, L. Kunze, S. Breimaier, M. Bolte, H.-W. Lerner, F. Jäkle, R. F. Winter, M. Braun, J.-M. Mewes and M. Wagner, Exploring Structure–Property Relations of B,S-Doped Polycyclic Aromatic Hydrocarbons through the Trinity of Synthesis, Spectroscopy, and Theory, *J. Am. Chem. Soc.*, 2022, **144**, 13704; (l) H. Luo, D. He, Y. Zhang, S. Wang, H. Gao, J. Yan, Y. Cao, Z. Cai, L. Tan, S. Wu, L. Wang and Z. Liu, Synthesis of Heterocyclic Core-Expanded Bis-Naphthalene Tetracarboxylic Diimides, *Org. Lett.*, 2019, **21**, 9734.
- 8 (a) J. B. Edson and D. M. Knauss, Thianthrene as an activating group for the synthesis of poly(aryl ether thianthrene)s by nucleophilic aromatic substitution, *Polym. Chem.*, 2004, **42**, 6353; (b) K. Fries, H. Koch, H. Slukenbrock and Z. K. des Thianthrens, *Justus Liebigs Ann. Chem.*, 1929, **468**, 162.
- 9 (a) O. A. Rakitin and L. S. Konstantinova, Chapter 4 Sulfur Monochloride in the Synthesis of Heterocyclic Compounds, *Adv. Heterocycl. Chem.*, 2008, **96**, 175; (b) T. Link, M. Oberjat and G. Klar, Dithiines Annulated by heterocycles. Part 2. Reaction of Disulfur Dichloride with Various Quinolines, *J. Chem. Res., Synop.*, 1997, 435; (c) F. Mostaghimi, E. Lork, I. Hong, T. L. Roemmele, R. T. Boéré, S. Mebs and J. Beckmann, The reaction of phenoxatellurine with single-electron oxidizers revisited, *New J. Chem.*, 2019, **43**, 12754; (d) A. Spurg, G. Schnakenburg and S. R. Waldvogel, Oxidative Coupling of Diaryldisulfides by MoCl<sub>5</sub> to Thianthrenes, *Chem. – Eur. J.*, 2009, **15**, 13313; (e) Z. S. Ariyan and R. L. Martin, Novel macrocyclic polysulfur compounds. 7,15,17,19-Tetra-alkoxy-2,3,4,5,10,11,12,13-octathiatricyclo-[12,2,2,2]eicosa-6,8,14,16,17,19-hexaenes and 2,3,7,8-tetra-alkoxythianthrens; products of the catalysed reaction of aromatic ethers and sulphur monochloride, *J. Chem. Soc., Perkin Trans. 1*, 1972, 1687; (f) S. Wang, J. Yuan, J. Xie, Z. Lu, L. Jiang, Y. Mu, Y. Huo, Y. Tsuchido and K. Zhu, Sulphur-Embedded Hydrocarbon Belts: Synthesis, Structure and Redox Chemistry of Cyclothianthrenes, *Angew. Chem., Int. Ed.*, 2021, **60**, 18443.
- 10 I. W. J. Still and V. A. Sayeed, A Versatile Synthetic Route to Substituted Thianthrenes, *Synth. Commun.*, 1983, **13**, 1181.
- 11 (a) P. Preedasuriyachai, P. Charoonniyomporn, O. Karoonnirun, T. Thongpanchang and Y. Thebtaranonth, A novel one-pot synthesis of derivatives of aryldioxins and aryldithiins, *Tetrahedron Lett.*, 2004, **45**, 1343; (b) C. Marti, J. Irurre, A. Alvarez-Larena, J. F. Piniella, E. Brillas, L. Fajari, C. Alemán and L. Juliá, Synthesis, Properties, and X-ray Structure of 6-Aza-5,7,12,14-tetrathiapentacene as a Novel Polyheterocyclic Electron Donor, and Related Compounds, *J. Org. Chem.*, 1994, **59**, 6200.
- 12 R. Sato, A. Onodera, T. Goto and M. Saito, Chemistry on Benzopentathiepin. Reactions of Benzopentathiepin with Aromatic Compounds in the Presence of Lewis Acid, *Heterocycles*, 1988, **27**, 2563.
- 13 (a) H. Ito, K. Ozaki and K. Itami, Annulative  $\pi$ -Extension (APEX): Rapid Access to Fused Arenes, Heteroarenes, and Nanographenes, *Angew. Chem., Int. Ed.*, 2017, **56**, 11144; (b) H. Ito, Y. Segawa, K. Murakami and K. Itami, Polycyclic Arene Synthesis by Annulative  $\pi$ -Extension, *J. Am. Chem. Soc.*, 2019, **141**, 3.
- 14 Our previous examples of APEX reactions: (a) K. Ozaki, K. Kawasumi, M. Shibata, H. Ito and K. Itami, One-shot K-region-selective annulative  $\pi$ -extension for nanographene synthesis and functionalization, *Nat. Commun.*, 2015, **6**,



- 6251; (b) W. Matsuoka, H. Ito and K. Itami, Rapid Access to Nanographenes and Fused Heteroaromatics by Palladium-Catalyzed Annulative  $\pi$ -Extension Reaction of Unfunctionalized Aromatics with Diiodobiaryls, *Angew. Chem., Int. Ed.*, 2017, **56**, 12224; (c) W. Matsuoka, H. Ito, D. Sarlah and K. Itami, Diversity-oriented synthesis of nanographenes enabled by dearomative annulative  $\pi$ -extension, *Nat. Commun.*, 2021, **12**, 3940; (d) T. Nakamuro, K. Kumazawa, H. Ito and K. Itami, Bay-Region-Selective Annulative  $\pi$ -Extension (APEX) of Perylene Diimides with Arynes, *Synlett*, 2019, **30**, 423; (e) K. Ozaki, K. Murai, W. Matsuoka, K. Kawasumi, H. Ito and K. Itami, One-Step Annulative  $\pi$ -Extension of Alkynes with Dibenzosiloles Dibenzogermoles by Palladium/o-chloranil Catalysis, *Angew. Chem., Int. Ed.*, 2017, **56**, 1361; (f) K. Ozaki, W. Matsuoka, H. Ito and K. Itami, Annulative  $\pi$ -Extension (APEX) of Heteroarenes with Dibenzosiloles and Dibenzogermoles by Palladium/o-Chloranil Catalysis, *Org. Lett.*, 2017, **19**, 1930; (g) H. Kitano, W. Matsuoka, H. Ito and K. Itami, Annulative  $\pi$ -extension of indoles and pyrroles with diiodobiaryls by Pd catalysis: rapid synthesis of nitrogen-containing polycyclic aromatic compounds, *Chem. Sci.*, 2018, **9**, 7556; (h) W. Matsuoka, K. P. Kawahara, H. Ito, D. Sarlah and K. Itami, *J. Am. Chem. Soc.*, 2023, **145**, 658.
- 15 Representative examples of the hetero-APEX reaction: (a) K. P. Kawahara, W. Matsuoka, H. Ito and K. Itami, Synthesis of Nitrogen-Containing Polyaromatics by Aza-Annulative  $\pi$ -Extension of Unfunctionalized Aromatics, *Angew. Chem., Int. Ed.*, 2020, **59**, 6383; (b) J. Yan, A. P. Pulis, G. J. P. Perry and D. J. Procter, Metal-Free Synthesis of Benzothiophenes by Twofold C–H Functionalization: Direct Access to Materials-Oriented Heteroaromatics, *Angew. Chem., Int. Ed.*, 2019, **58**, 15675; (c) E. Schendera, L.-N. Unkel, P. P. H. Quyen, G. Salkewitz, F. Hoffmann, A. Villinger and M. Brasholz, Visible-Light-Mediated Aerobic Tandem Dehydrogenative Povarov/Aromatization Reaction: Synthesis of Isocryptolepines, *Chem. – Eur. J.*, 2020, **26**, 269; (d) Z. Yu, Y. Zhang, J. Tang, L. Zhang, Q. Liu, Q. Li, G. Gao and J. You, Ir-Catalyzed Cascade C–H Fusion of Aldoxime Ethers and Heteroarenes: Scope and Mechanisms, *ACS Catal.*, 2020, **10**, 203; (e) S. Tokita, K. Hiruta, K. Kitahara and H. Nishi, Diels-Alder Reaction of Dialkyl Diazenedicarboxylates with Perylenes; A New Synthesis of Polycyclic Aromatic Pyridazines, *Synthesis*, 1982, 229; (f) S. Maiti, T. K. Achar and P. Mal, An Organic Intermolecular Dehydrogenative Annulation Reaction, *Org. Lett.*, 2017, **19**, 2006; (g) R. Regar, R. Mishra, P. K. Mondal and J. Sankar, Metal-free Annulation at the Ortho- and Bay-Positions of Perylene Bisimide Leading to Lateral  $\pi$ -Extension with Strong NIR Absorption, *J. Org. Chem.*, 2018, **83**, 9547; (h) Y. Tokimaru, S. Ito and K. Nozaki, Synthesis of Pyrrole-Fused Corannulenes: 1,3-Dipolar Cycloaddition of Azomethine Ylides to Corannulene, *Angew. Chem., Int. Ed.*, 2017, **56**, 15560; (i) A. Qarah, M. Gasonoo, D. Do and D. A. Klumpp, Superacid-promoted synthesis of polychlorinated dibenzofurans, *Tetrahedron Lett.*, 2016, **57**, 3711; (j) C. Chen, Y. Wang, X. Shi, W. Sun, J. Zhao, Y.-P. Zhu, L. Liu and B. Zhu, Palladium-Catalyzed C-2 and C-3 Dual C–H Functionalization of Indoles: Synthesis of Fluorinated Isocryptolepine Analogues, *Org. Lett.*, 2020, **22**, 4097; (k) M. Wang, L. Kong, F. Wang and X. Li, Rhodium-Catalyzed Amination and Annulation of Arenes with Anthranils: C–H Activation Assisted by Weakly Coordinating Amides, *Adv. Synth. Catal.*, 2017, **359**, 4411; (l) A. V. Aksenov, N. A. Aksenov, A. S. Lyakhovnenko and I. V. Aksenova, Regioselectivity Change in the Reaction of Naphthalene and 2-Naphthyl Ethers with 1,3,5-Triazines Depending on Reagent Quantities, *Synthesis*, 2009, 3439; (m) M. A. Bashir, Y. Zhang, H. Yu, B. Wang, W. Zhao and F. Zhong, Bimetallic copper/cobalt-cocatalyzed double aerobic phenol oxidation/cyclization toward  $\pi$ -extended benzofuro[2,3-b]indoles as electron donors for electroluminescence, *Green Chem.*, 2021, **23**, 5031; (n) S. C. Benson, J. L. Gross and J. K. Snyder, Indole as a dienophile in inverse electron demand Diels-Alder reactions: reactions with 1,2,4-triazines and 1,2-diazines, *J. Org. Chem.*, 1990, **55**, 3257; (o) K. P. Kawahara, W. Matsuoka, H. Ito and K. Itami, Rapid access to polycyclic thiopyrylium compounds from unfunctionalized aromatics by thia-APEX reaction, *Chem. Commun.*, 2023, **59**, 1157.
- 16 (a) F. Masetti and U. Mazzucato, Heavy atom effect on the luminescence of phenanthrene, *J. Lumin.*, 1971, **4**, 8; (b) C. A. Parker and C. G. Hatchard, *Analyst*, 1962, **87**, 664; (c) S. Kyushin, H. Fujii, K. Negishi and H. Matsumoto, Improvement of the fluorescence quantum yield of triphenylene by the rotational effect of 4-(trimethylsilyl)phenyl groups, *Mendeleev Commun.*, 2022, **32**, 87.
- 17 The fluorescent quantum yields of the commercially available pristine phenanthrene and corannulene in  $\text{CH}_2\text{Cl}_2$  were measured using a spectrofluorophotometer in our laboratory (see the ESI<sup>†</sup>), and determined to be 3% and 1%, respectively. These values were lower than those reported in the literature (14% and 7%): ref. 16a and b and J. Mack, P. Vogel, D. Jones, N. Kavala and A. Suttona, The development of corannulene-based blue emitters, *Org. Biomol. Chem.*, 2007, **5**, 2448.
- 18 M. J. Frisch, G. W. Trucks, H. B. Schlegel, G. E. Scuseria, M. A. Robb, J. R. Cheeseman, G. Scalmani, V. Barone, G. A. Petersson, H. Nakatsuji, X. Li, M. Caricato, A. V. Marenich, J. Bloino, B. G. Janesko, R. Gomperts, B. Mennucci, H. P. Hratchian, J. V. Ortiz, A. F. Izmaylov, J. L. Sonnenberg, D. Williams-Young, F. Ding, F. Lipparini, F. Egidi, J. Goings, B. Peng, A. Petrone, T. Henderson, D. Ranasinghe, V. G. Zakrzewski, J. Gao, N. Rega, G. Zheng, W. Liang, M. Hada, M. Ehara, K. Toyota, R. Fukuda, J. Hasegawa, M. Ishida, T. Nakajima, Y. Honda, O. Kitao, H. Nakai, T. Vreven, K. Throssell, J. A. Montgomery Jr., J. E. Peralta, F. Ogliaro, M. J. Bearpark, J. J. Heyd, E. N. Brothers, K. N. Kudin, V. N. Staroverov, T. A. Keith, R. Kobayashi, J. Normand, K. Raghavachari, A. P. Rendell, J. C. Burant, S. S. Iyengar, J. Tomasi, M. Cossi,



- J. M. Millam, M. Klene, C. Adamo, R. Cammi, J. W. Ochterski, R. L. Martin, K. Morokuma, O. Farkas, J. B. Foresman and D. J. Fox, *Gaussian 16, Revision C.01*, Gaussian, Inc., Wallingford, CT, 2016.
- 19 (a) A. D. Becke, Density-functional thermochemistry. III. The role of exact exchange, *J. Chem. Phys.*, 1993, **98**, 5648; (b) C. Lee, W. Yang and R. G. Parr, Development of the Colle-Salvetti correlation-energy formula into a functional of the electron density, *Phys. Rev. B: Condens. Matter Mater. Phys.*, 1988, **37**, 785.
- 20 B. Mennucci, E. Cancès and J. Tomasi, Evaluation of Solvent Effects in Isotropic and Anisotropic Dielectrics and in Ionic Solutions with a Unified Integral Equation Method: Theoretical Bases, Computational Implementation, and Numerical Applications, *J. Phys. Chem. B*, 1997, **101**, 10506.
- 21 The commonly known range of interplanar distances by  $\pi$ - $\pi$  stacking is 3.3–3.8 Å according to a reference: C. J. Janiak, A critical account on  $\pi$ - $\pi$  stacking in metal complexes with aromatic nitrogen-containing ligands, *Chem. Soc., Dalton Trans.*, 2000, 3885.
- 22 (a) I. Rowe and B. Post, The crystal structure of thianthrene, *Acta Crystallogr.*, 1958, **11**, 372; (b) H. Lynton and E. G. Cox, The crystal and molecular structure of thianthrene, *J. Chem. Soc.*, 1956, 4886.
- 23 (a) M. Nishio, *CrystEngComm*, 2004, **6**, 130; (b) G. Aragay, D. Hernández, B. Verdejo, E. C. Escudero-Adán, M. Martínez and P. Ballester, Quantification of CH- $\pi$  Interactions Using Calix[4]pyrrole Receptors as Model Systems, *Molecules*, 2015, **20**, 16672.
- 24 (a) E. R. Johnson, S. Keinan, P. Mori-Sánchez, J. Contreras-García, A. J. Cohen and W. Yang, Revealing Noncovalent Interactions, *J. Am. Chem. Soc.*, 2010, **132**, 6498; (b) J. Contreras-García, E. R. Johnson, S. Keinan, R. Chaudret, J.-P. Piquemal, D. N. Beratan and W. Yang, NCIPLOT: A Program for Plotting Noncovalent Interaction Regions, *J. Chem. Theory Comput.*, 2011, **7**, 625; (c) R. A. Boto, F. Peccati, R. Laplaza, C. Quan, A. Carbone, J.-P. Piquemal, Y. Maday and J. Contreras-García, NCIPLOT4: Fast, Robust, and Quantitative Analysis of Noncovalent Interactions, *J. Chem. Theory Comput.*, 2020, **16**, 4150.
- 25 (a) S. Sanyal, A. K. Manna and S. K. Pati, Functional Corannulene: Diverse Structures, Enhanced Charge Transport, and Tunable Optoelectronic Properties, *ChemPhysChem*, 2014, **15**, 885; (b) T. Guo, A. Li, J. Xu, K. K. Baldrige and J. Siegel, Enantiopure C5 Pentaindenocorannulenes: Chiral Graphenoid Materials, *Angew. Chem., Int. Ed.*, 2021, **60**, 25809; (c) B. M. Schmidt, B. Topolinski, P. Roesch and D. Lentz, Electron-poor N-substituted imide-fused corannulenes, *Chem. Commun.*, 2012, **48**, 6520; (d) A. Steinauer, A. M. Butterfield, A. Linden, A. Molina-Ontario, D. C. Buck, R. W. Cotta, L. Echegoyen, K. K. Baldrige and J. S. Siegel, Tunable Photochemical/Redox Properties of (Phenylthio)ncorannulenes: Application to a Photovoltaic Device, *J. Braz. Chem. Soc.*, 2016, **27**, 1866; (e) Non-substituted corannulene is favored to form a disordered close-packed structure according to this paper: R. L. Parc, P. Hermet, S. Rols, D. Maurin, L. Alvarez, A. Ivanov, J. M. Quimby, C. G. Hanley, L. T. Scott and J.-L. Bantignies, New Insights on Vibrational Dynamics of Corannulene, *J. Phys. Chem. C*, 2012, **116**, 25089.
- 26 (a) R. Chen, R.-Q. Lu, P.-C. Shi and X.-Y. Cao, Corannulene derivatives for organic electronics: From molecular engineering to applications, *Chin. Chem. Lett.*, 2016, **27**, 1175; (b) X. Chena, H. Wanga, B. Wanga, Y. Wanga, X. Jinb and F.-Q. Bai, Charge transport properties in organic D-A mixed-stack complexes based on corannulene and sumanene derivatives—a theoretical study, *Org. Electron.*, 2019, **68**, 35; (c) K. Menekse, R. Renner, B. Mahlmeistera, M. Stoltea and F. Würthner, Bowl-Shaped Naphthalimide-Annulated Corannulene as Nonfullerene Acceptor in Organic Solar Cells, *Org. Mater.*, 2020, **2**, 229.
- 27 (a) J. Kang, D. Miyajima, T. Mori, Y. Inoue, Y. Itoh and T. Aida, Noncovalent assembly. A rational strategy for the realization of chain-growth supramolecular polymerization, *Science*, 2015, **347**, 646; (b) D. Miyajima, K. Tashiro, F. Araoka, H. Takezoe, J. Kim, K. Kato, M. Takata and T. Aida, Liquid Crystalline Corannulene Responsive to Electric Field, *J. Am. Chem. Soc.*, 2009, **131**, 44.
- 28 (a) S. Kim, Y. Kwon, J.-P. Lee, S.-Y. Choi and J. Choo, A theoretical investigation into the conformational changes of dibenzo-p-dioxin, thianthrene, and selenanthrene, *J. Mol. Struct.*, 2003, **655**, 451; (b) J. Chickos and K. Mislow, Conformational Flexibility of Thianthrene and Its Oxides, *J. Am. Chem. Soc.*, 1967, **89**, 4815.
- 29 P. U. Biedermann, S. Pogodin and I. Agranat, Inversion Barrier of Corannulene. A Benchmark for Bowl-to-Bowl Inversions in Fullerene Fragments, *J. Org. Chem.*, 1999, **64**, 3655.

